FOREX Publication
Open Access | Rapid and quality publishing

International Journal of
Electrical and Electronics Research (IJEER)
Research Article | Volume 10, Issue 4 | Pages 1058-1063 | e-ISSN: 2347-470X

High Gain Converter Design and Implementation for Electric Vehicles

Jayanthi Kathiresan[1*] and Gnanavadivel Jothimani[2]
[1,2]Mepco Schlenk Engineering College, Sivakasi; [1]kjayanthi@mepcoeng.ac.in, [2]gvadivel@mepcoeng.ac.in

***Correspondence:** Jayanthi Kathiresan; kjayanthi@mepcoeng.ac.in; Tel.: +91-9944791506

ABSTRACT- In this paper, a new Single Ended Primary Inductance Converter based dc- dc converter operate in boost converter mode is proposed. The converter is designed by incorporating the quasi-Z source structure and switched capacitor cell. The salient features of the proposed converter are high range of voltage gain, less voltage stress across the semiconductor devices and high efficiency. This characteristic creates the high gain converter an exceptional interface among the dc source and the load inside the electric vehicle. The steady state analysis of this topology in continual operating mode and the transient behavior are analyzed. Finally, a prototype of the converter 100W/200V is fabricated to confirm the practicability with conceptual analysis of the high gain converter.

Keywords: SEPIC; Switched Capacitor Cell; Quasi Z source network.

ARTICLE INFORMATION

Author(s): Jayanthi Kathiresan and Gnanavadivel Jothimani;
Received: 29/09/2022; **Accepted**: 07/11/2022; **Published**: 20/11/2022;
e-ISSN: 2347-470X;
Paper Id: IJEER 2909-52;
Citation: 10.37391/IJEER.100449
Webpage-link:
www.ijeer.forexjournal.co.in/archive/volume-10/ijeer-100449.html

Publisher's Note: FOREX Publication stays neutral with regard to Jurisdictional claims in Published maps and institutional affiliations.

1. INTRODUCTION

Traditional fossil fuels contribute to increased pollution due to their continuous use. Electric vehicles use DC-DC converters to distribute power from batteries to their components. [1]. With a step-up converter structure, the low-level voltage is converted to the higher voltage level for the moment storing the input energy, which is later de-energized at the higher voltage level. The storage of energy in magnetic or electric fields can be accomplished by using various active or passive switching components such as single or coupled inductors or capacitors [2]. Boost converters use a low ripple current as an input, but their voltage gain is limited and their power electronic switches are under high voltage stress. It provides the voltage conversion both up and down (step-up and step-down) in many different types of converters, including conventional converters like buck-boost converters and CUK converters [3]. When the duty cycle of this type of converter reaches unity, the efficiency and static gain are greatly reduced due to an increase in conduction and power electronic switch losses.

The multi-level DC-DC Boost converter achieves high potential gain and provides low stress across power semiconductors. Three-level step-up converters (3LB) are of great interest because of the low voltage stress applied across semiconductor devices [4]. Because of the level three DC-DC converters necessitates a complex control switching to maintain the capacitor voltage. The conventional Boost level 2 DC-DC converter is a converter that share a ground as common, but their voltage-gain is still has restriction. It is used because of its simple structure; it has disadvantages like limited static gain and voltage stress on its semiconductors will be high [5].

Non-coupled converters are based on boost converter in conjunction with voltage multipliers in the form of switched-inductor or switched-capacitor cells. Because of their large number of components, the efficiency can be low, mainly when the several voltage multiplier stages were used [6]. The step up high gain converter topologies also works in conjunction with a qZs network. Coupled inductor based high gain converters are used to provide high voltage gain in DC-DC converters by adjusting the transformer winding ratio. As a result, the operating duty ratio and voltage stress across the semiconductors rises. It is possible to clamp the voltage using energy regenerating techniques in these converters, which increase the cost, complexity, and reduce the efficiency [7].

In addition to cascaded, multilevel, and interleaved topologies, other methods are also used to augment the static voltage gain of converters. These methods increase the gain in a linear or exponential way, depending on the topology [8]. Z source converters are high voltage gain converters, but they lack a common ground between the input and output sides, which may cause maintenance issues and additional EMI cost. This type of step up converter also causes extreme voltage stresses on the semiconductor devices [9]. To generate an adequate DC bus voltage level, the converters must have more voltage gain [10]. If the above said converters are interfaced with the renewable sources such as solar PV panel, fuel cell etc., and the output voltage from these sources are very low, then the converters has to boost and regulates the output voltage. The above said converters suffer a lot of issues in terms of voltage stress, voltage gain, and efficiency and control methods [11, 12]. The SEPIC converter topology is presented in [17] designed to get dual output voltage and finds suitable for PV applications. The modified SEPIC based DC-DC converter was developed using switched inductor method is presented in [18]. The converter is

FOREX Publication
Open Access | Rapid and quality publishing
International Journal of Electrical and Electronics Research (IJEER)
Research Article | Volume 10, Issue 4 | Pages 1058-1063 | e-ISSN: 2347-470X

designed to improve the voltage gain. The high gain boost converter is designed to improve the voltage gain is presented in [19, 20].

To address the above issues a non-isolated DC-DC power converter is developed to boost the output voltage by employing voltage boosting techniques such as switched capacitor, quasi-Z source network etc., in the existing converter topology. The addition of voltage boosting technique in the converter increases the voltage gain as well as the efficiency and source current continuous, making it especially suitable for electric vehicle applications.

2. DESIGNED CONVERTER TOPOLOGY AND ITS OPERATING MODES

The developed High Gain Converter consists of power switch as Q, five number of power diodes as D_1, D_2, D_3, D_4, D_5, seven number of capacitors as C_1 *to* C_7, and three inductive elements represented as L_1, L_2, L_3. The converter analysis is done by using resistive load. The converter is developed by keeping the switch Q, inductor L_1 in the input side, diode $D_1$and capacitor C_6 at the output side of the SEPIC. The load side inductor of the SEPIC is replaced by a quasi-Z source set-up comprising of inductors and capacitors L_2, D_2, C_2, C_7. A switched-capacitor networks with the diodes and capacitors D_3, D_4, D_5 & C_3, C_4, C_5 is added to augment the voltage gain. The circuit diagram and the corresponding switching waveforms are shown in *figure 1 and 2(a) & (b).*

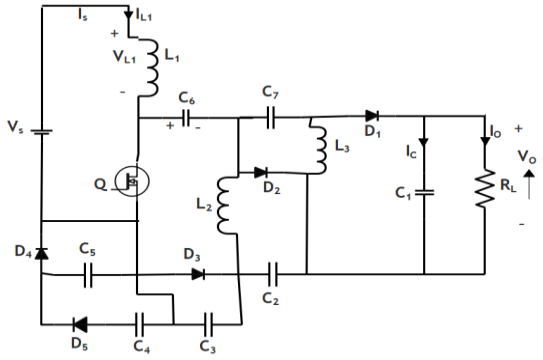

Figure 1: Circuit diagram of High Gain converter

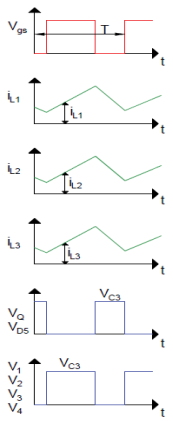

Figure 2(a): Switching Waveforms of High Gain converter

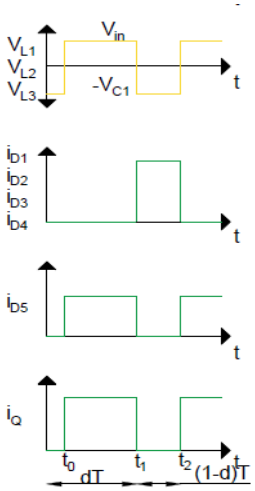

Figure 2(b): Switching Waveforms of High Gain converter

The designed DC-DC converter has two switching states. During ON condition the power switch Q is in conduction state, the diodes $D_1, to\ D_4$ are in off condition and power diode D_5 is in ON condition. In this case, the C_1, C_2, C_5 & C_3 capacitors discharge its energy and the C_7, C_6, and C_4 capacitors get charged. The circuit diagram during turns ON state is shown in *figure 3*. The following *equations (1-4)* have been derived by using the Kirchhoff Voltage Law.

$$U_{L1} = U_s \quad (1)$$

$$U_{L2} = U_{C3} - U_{C6} \quad (2)$$

$$U_{L3} = U_{C3} - U_{C6} + U_{C7} \quad (3)$$

$$U_{C5} = U_{C4} \quad (4)$$

In OFF state, the power switch Q is in off mode, the diodes D_1, D_2, D_3, D_4 are in ON condition, and D_5 is in off condition. The capacitorsC_1, C_2, C_3,& C_5 gets charged and the capacitors C_4, C_6, & C_7 discharges. *Figure 4* shows the current flowing direction during turn OFF state. By using the KVL to the *figure 4*, the subsequent equations have been derived:

$$U_{L1} = U_s - U_{C3} \quad (5)$$

$$U_{L1} = U_s - U_{C5} \quad (6)$$

$$U_{L2} = -U_{C2} \quad (7)$$

$$U_{L2} = -U_{C6} \quad (8)$$

$$U_{L3} = -U_{C1} \quad (9)$$

Voltage-Second balance rule is used to the inductive element voltages during ON state periods & OFF state periods for obtaining the static voltage gain of the high gain converter. Using the *equations (1 & 5)* in *equation (10)*, the following *equations (11)* is obtained.

$$\int_{to}^{t1} U_{L1} dt^I + \int_{t1}^{t2} U_{L1} dt^{II} = 0 \quad (10)$$

FOREX Publication
Open Access | Rapid and quality publishing
International Journal of Electrical and Electronics Research (IJEER)
Research Article | Volume 10, Issue 4 | Pages 1058-1063 | e-ISSN: 2347-470X

$$M_O = \frac{U_o}{U_s} = \frac{(2+2d)}{(1-d)} \quad (11)$$

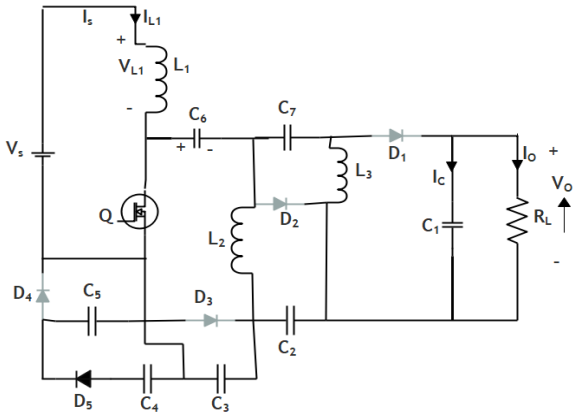

Figure 3: Current Direction during turn ON state

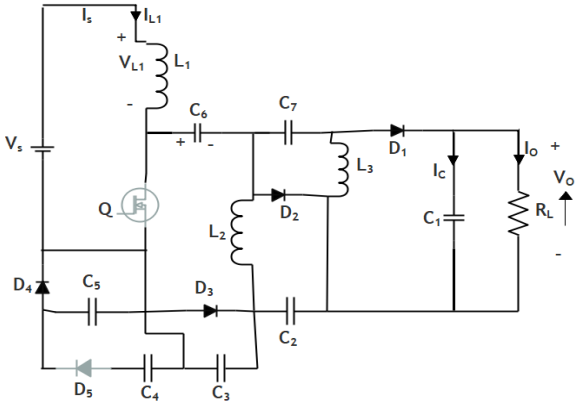

Figure 4: Current direction during turn OFF state

3. COMPONENT

3.1 Design of Inductor

The value of inductorsL_1, L_2 , L_3 used in this converter depends on duty ratio d, switching frequency fs, supply voltage U_{in} and ripple currents Δi_{L1} , Δi_{L2} , Δi_{L3}. The values are calculated by using the *equations (12-14).*

$$L_1 = \frac{dU_{in}}{f_s \Delta i_{L1}} \quad (12)$$

$$L_2 = \frac{dU_{in}}{f_s \Delta i_{L2}} \quad (13)$$

$$L_3 = \frac{dU_{in}}{f_s \Delta i_{L3}} \quad (14)$$

3.2 Selection of Capacitor

There are seven capacitors $C_1, C_2, C_3, C_4, C_5, C_6, C_7$ used in this converter. By calculating the maximum ripple voltages ΔU_{C1}, ΔU_{C2}, ΔU_{C3}, ΔU_{C4}, ΔU_{C5}, ΔU_{C6} and ΔU_{C7}, we can determine all the seven capacitor values by using equations (15 to 21), where the duty cycle is represented as d, switching frequency is represented as f_s and the output current of the converter is I_o.

$$C_1 = \frac{I_o d}{f_s \Delta U_{C1}} \quad (15)$$

$$C_2 = \frac{2I_o d}{f_s \Delta U_{C2}} \quad (16)$$

$$C_3 = \frac{3I_o d}{f_s \Delta U_{C3}} \quad (17)$$

$$C_4 = \frac{I_o (1-d)}{f_s \Delta U_{C4}} \quad (18)$$

$$C_5 = \frac{I_o d}{f_s \Delta U_{C5}} \quad (19)$$

$$C_6 = \frac{2I_o d}{f_s \Delta U_{C6}} \quad (20)$$

$$C_7 = \frac{I_o d}{f_s \Delta U_{C7}} \quad (21)$$

4. COMPARATIVE ANALYSIS OF DESIGNED HIGH GAIN CONVERTER WITH EXISTING CONVERTER TECHNOLOGY

The designed high gain converter is evaluate with the other converters in terms of voltage gain, amount of elements in the power circuit, input current ripple etc. The developed converter voltage gain is between 2 to 38 for the duty ratio of 0 to 0.9 which is high when compared to the converters presented in [2, 13]. When compared with [11], the number power switches and power diodes are less in developed converter topology. Similarly, the input current ripple in [11] is high when compared with the designed High gain converter topology. This reduced current ripple makes the converter suitable for renewable energy based electric vehicle systems.

Table 1: High Gain converter comparison with other converters in the literature

Topology	Voltage Gain	Number of switches & diode	Number of inductors & capacitors	Input current ripple
[2]	1/1-d	2 , 2	1,2	Minimum
[4]	2/1-d	2,3	2,3	Minimum
[11]	(1+5d)/(1-d)	3,12	6,1	Maximum
[13]	1/d(1-d)	2,3	2,2	Minimum
Proposed	(2+2d)/(1-d)	1,5	3,7	Minimum

5. RESULTS AND DISCUSSION

The high gain converter circuit parameters are designed by using the above equations and the power converter is designed to handle the 24V source voltage, 200V load voltage and 100W of load power. The parameters and its values considered for the simulation and experimental prototype is tabulated in *table 2* and the MATLAB simulated structure is depicts in *figure 5*. The high gain converter's load voltage is regulated and maintained by using PI controller. The PI controller parameters k_p and k_i

FOREX Publication
Open Access | Rapid and quality publishing
International Journal of Electrical and Electronics Research (IJEER)
Research Article | Volume 10, Issue 4 | Pages 1058-1063 | e-ISSN: 2347-470X

are tuned by using Z-N method and the obtained values are 0.0123 and 0.786 respectively. In the closed loop mode the controller generates the control signal based on the computed error value from the variations in load voltage and set point voltage. That control signal is used to operate the power switch to retain the load voltage of 200V. The closed loop simulated waveforms of voltage and current on the input and load side of the topology are shown in *figure 6.* The controller takes less than 0.02s to regulate and maintains the load voltage of 200V.

The performance of the high gain converter with the controller is analyzed for the variation in reference voltage. The reference voltage is varied from 20V above the reference voltage (220 V) and 20V below the reference voltage (180 V). The simulated graphical representation of the variation is shown in *figure 6a*.

To validate the simulated results, the experimental hardware prototype model is developed for 24 V at the source side, 200 V at the output end of the converter and the load power of 100W and is depicted in *figure 7.* The required gating pulse for the converter operation is generated by using PIC 18F452 series microcontroller. The duty ratio of 0.65 is required to get the load voltage of 200 V for the given input of 24 V. The gating signal waveform generated using microcontroller is pictured in *figure 8. Figure 9 (a) & (b)* shows the experimental load voltage waveform obtained from high gain converter for the input voltage of 10V and 24 V. The PI controller employed in the converter maintained the load voltage of 100 V and 200 V for the corresponding input voltage. The current waveforms of the inductive elements L_1, L_2 and L_3 are obtained and shown in *figure 10 (a), (b) &(c).* The theoretical and simulated results are validated in the experimental model. On comparing the simulated and experimental values of output voltage about 100V & 200V are maintained.

Table 2: Experimental and Simulated Parameters

Parameters	Value
Source Voltage	10 V – 24 V
Load Voltage	200 V
Load Power	100 W
Switching Frequency	20kHz
Inductance	L_1= 357 µH, L_2 = L_3 = 478 µH
Capacitor	C_1 = C_7= 47 µF, C_2 = C_6= 47 µF,C_3 = C_4 = C_5= 100 µF
Diode	MBR3060PT
Power Switch	IRF240 V

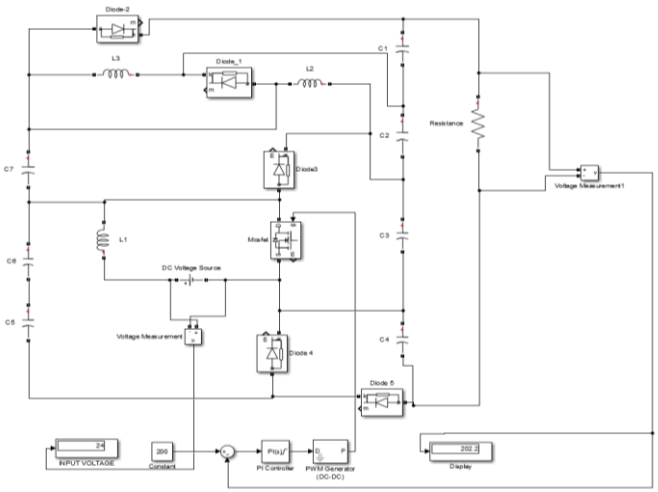

Figure 5: MATLAB Simulated High Gain Converter Structure

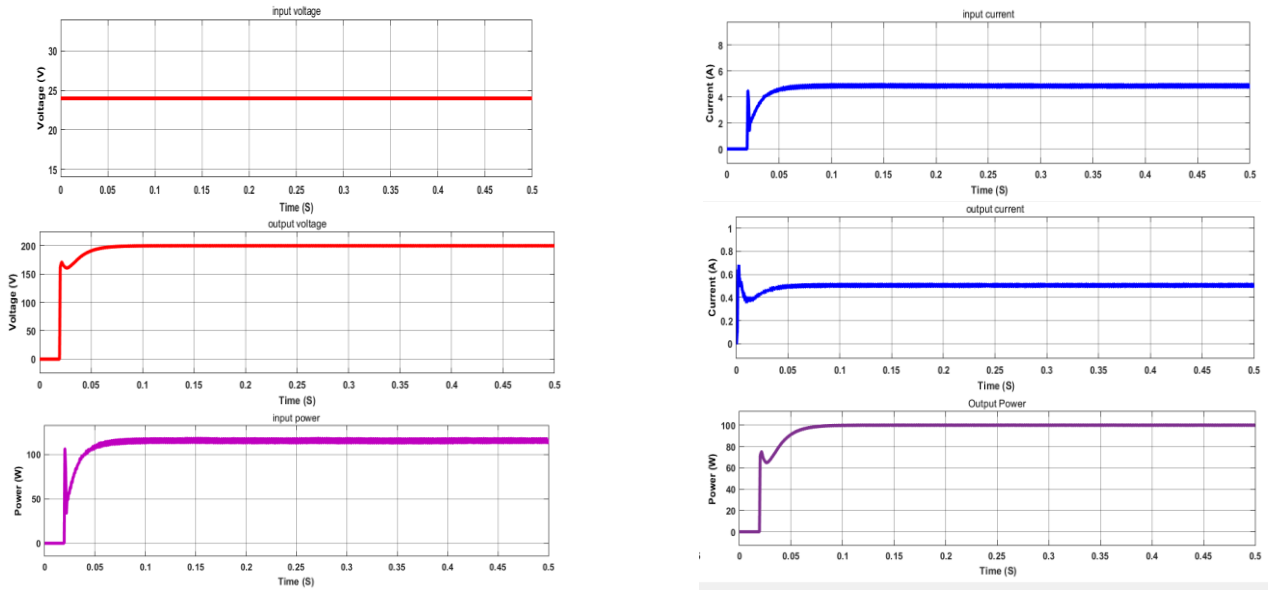

Figure 6: Closed loop Simulated waveforms of Input and Output voltage, current and Power Parameters

FOREX Publication
Open Access | Rapid and quality publishing
International Journal of Electrical and Electronics Research (IJEER)
Research Article | Volume 10, Issue 4 | Pages 1058-1063 | e-ISSN: 2347-470X

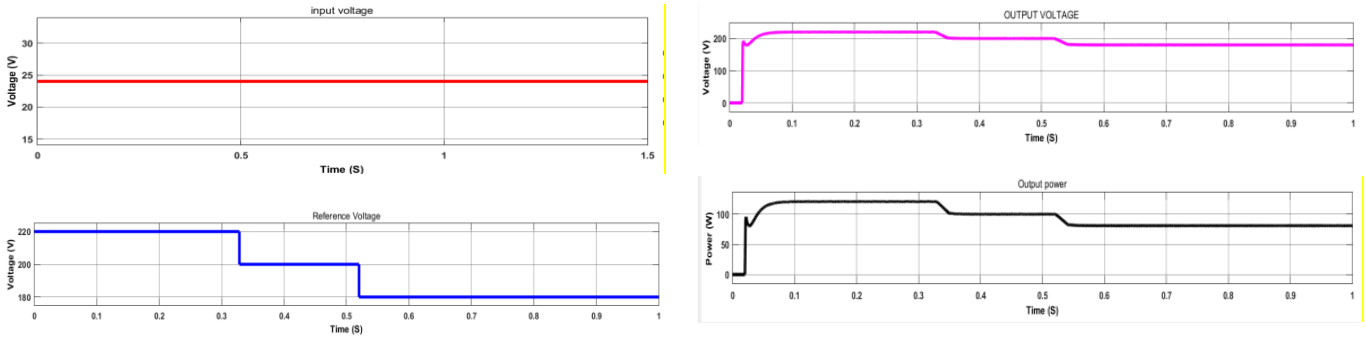

Figure 6a: Transient Simulated waveforms of Input and Output Voltage, Reference Voltage and Output Power under Reference Voltage variation

Figure 7: Experimental Prototype Model of High Gain Converter

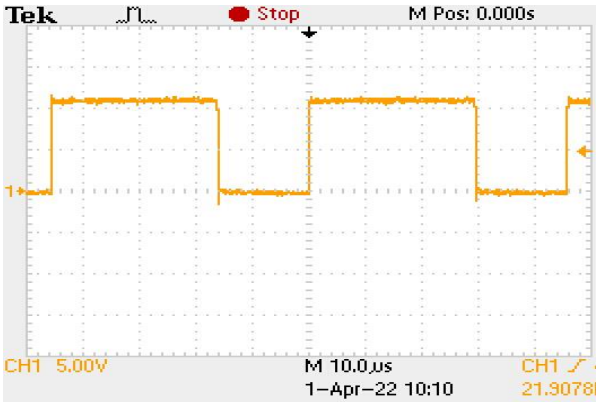

Figure 8: Gating Signal for the Power Switch

Figure 9(a): Experimental Output Voltage waveform for the input voltage of 10 V

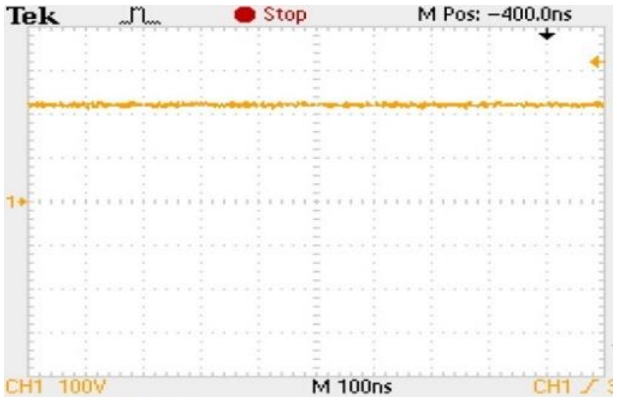

Figure 9(b): Experimental Output Voltage waveform for the input voltage of 24 V

(a)

(b)

FOREX Publication
Open Access | Rapid and quality publishing
International Journal of Electrical and Electronics Research (IJEER)
Research Article | Volume 10, Issue 4 | Pages 1058-1063 | e-ISSN: 2347-470X

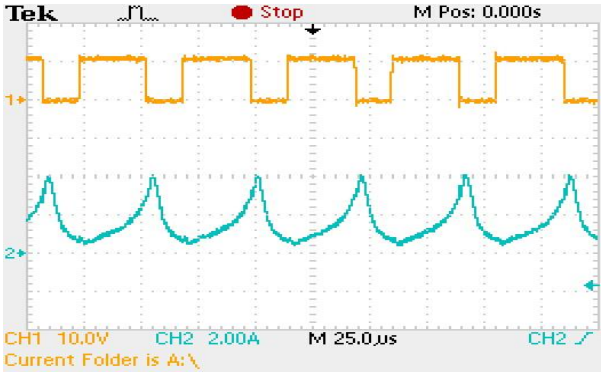

(c)

Figure 10: Inductor Current Waveforms (a) Inductor L_1; (b) Inductor L_2; (c) Inductor L_3

6. CONCLUSION

A high gain converter by means of a qZs and switched capacitor has been designed to augment the static voltage gain. By using the designed topology, a continuous source current can be provided and a reduction in voltage stress can be achieved across power devices. The steady-state behavior of the converter in various operating modes is examined in this paper. In this study, simulations are conducted using an input voltage of 24V and an output voltage of 200V for the converter. Regulation of load voltage is achieved using the Proportional-Integral controller. This converter has a static gain of 10 for the given voltage and achieved an efficiency of 92% under rated conditions. Hardware experimental prototype models are developed to validate simulated results. The experimental efficiency of the designed converter at rated load condition is found to be 91.6%. Based on simulations and experiments, the designed converter appears to be a viable choice for electrical vehicles.

Author Contributions: "Conceptualization, Jayanthi. and Gnanavadivel; methodology, Gnanavadivel.; software, Jayanthi.; validation, Gnanavadivel and Jayanthi; formal analysis, Jayanthi & Gnanavadivel.; investigation, Gnanavadivel & Jayanthi.; writing—original draft preparation, Jayanthi.; writing—review and editing, Gnanavadivel.; All authors have read and agreed to the published version of the manuscript".

Conflicts of Interest: "The authors declare no conflict of interest."

REFERENCES

[1] Marcos Antonio Salvador,Telles Brunelli Lazzarin, Roberto Francisco Coelho. High Step-Up DC-DC Converter with Active Switched-Inductor and Passive Switched Capacitor Networks. IEEE Trans. Ind. Electron. 2018, 65, 5644-5654.

[2] Nour Elsayad, Hadi Moradisizkoohi. Analysis and implementation of a new SEPIC-based single switch buck-boost dc-dc converter with continuous input current. IEEE Trans. Power Electron. 2018,33,10317-10325.

[3] Yun Zhan, Jilong Shi, Lei Zhou, Jing Li, Mark Sumner, Ping Wing, and Changliang Xia. Wide Input Voltage Range Boost Three-Level DC-DC Converter with Quasi-Z Source for Fuel Cell Vehicles. IEEE Trans. Power Electron.2017,32,6728- 6738.

[4] J. Gnanavadivel, Kumar, N. S., and Yogalakshmi, P. Implementation of FPGA based three-level converter for LED drive applications. J. Optoelectron. Adv. Mater, 2016,18, 459-467.

[5] Ping Wang.; Lei Zhou, Yun Zhang, Jing Li. and Mark Sumner. Input-parallel Output-series DC-DC Boost Converter with a Wide Input Voltage Range, for Fuel Cell Vehicles. IEEE Trans. Veh. Technol. 2017, 66, 7771-7781.

[6] G. N. Ango, T. Roy, and P. K. Sadhu. A novel switched capacitor-based multilevel inverter structure for renewable energy conversion system. International Journal of Power Electronics. 2022,16,1–33.

[7] Mojtaba Forouzesh, Yam P. Siwakoti, Saman A. Gorji, Frede Blaabjerg and Brad Lehman. Step-Up DC–DC Converters: A Comprehensive Review of Voltage-Boosting Techniques, Topologies, and Applications. IEEE Transactions on Power Electronics, 2017, 32, 9143-9178.

[8] A.Tomaszuk and A. Krupa. High efficiency high step-up DC/DC converters – a review. Bulletin of The Polish Academy of Sciences Technical Sciences, 2011, 59, 475-483.

[9] N. Elsayad, H. Moradisizkoohi and O. A. Mohamme., Design and Implementation of a New Transformerless Bidirectional DC–DC Converter with Wide Conversion Ratios. IEEE Transactions on Industrial Electronics. 2019, 66, 7067-7077.

[10] R. Moradpour, H. Ardi and A. Tavakol. Design and Implementation of a New SEPIC-Based High Step-Up DC/DC Converter for Renewable Energy Applications. IEEE Transactions on Industrial Electronics. 2018, 65, 1290-1297.

[11] M. Srivastava, A. K. Verma and P. S. Tomar. A comparison of different DC-DC converter topology for electric vehicle charging. International Journal of Power Electronics, 2021, 13, 21–44.

[12] E. Babaei, H. M. Maheri, M. Sabahi, and S. H. Hosseini. Extendable Nonisolated High Gain DC–DC Converter Based on Active–Passive Inductor Cells. IEEE Trans. Ind. Electron., 2018,65, 9478 – 9487.

[13] Y. M. Ye, and K. W. E. Cheng. Quadratic boost converter with low buffer capacitor stress. IET Pow. Electron, 2014, 7, 1162 – 1170.

[14] F. M. Shahir, E. Babaei and M. Farsad., Extended Topology for a Boost DC–DC Converter. IEEE Transactions on Power Electronics. 2019, 34, 2375-2384.

[15] M. R. Banaei, S. G. Sani, "Analysis and Implementation of a New SEPIC-Based Single-Switch Buck–Boost DC–DC Converter with Continuous Input Current," IEEE Trans. Power. Electron. 2018, 33, 10317 – 10325.

[16] M. A. Salvador, T. B. Lazzarin, and R. F. Coelho. High Step-Up DC– DC Converter With Active Switched-Inductor and Passive Switched-Capacitor Networks. IEEE Trans. on Ind. Electron., 2018, 65, 5644 – 5654.

[17] N.Rathina Prabha, J. Gnanavadivel, and KS Krishna Veni. Performance Investigation of Single Switch Dual Output DC-DC SEPIC Converter for PV Applications. Int. J. Adv. Sci. Technol.; 2020,29, 4676-4683.

[18] K.Jayanthi, N.Senthil Kumar, and J.Gnanavadivel. Design and implementation of modified SEPIC high gain DC-DC converter for DC microgrid applications. Int. Trans. Electr. Energy Syst. ., 2021, 31, 2100-2118.

[19] M.Kalarathi, and K.Jayanthi. A Solar PV Fed Switched Capacitor Boost Circuit for DC Microgrid. Int. Trans. Electr. Energy Syst. ., 2021, 31, 2100-2118.

[20] B Abinayalakshmi, S. Muralidharan; and J. Gnanavadivel. Design of Quadratic Boost Converter for Renewable Applications. International Conference on Power Electronics and Renewable Energy Systems, 2022, 331-340.